Sparse Low-rank Component Based Representation for Face Recognition with Low Quality Images

Shicheng Yang, Le Zhang, Lianghua He*, and Ying Wen*

Abstract—Sparse-representation based classification (SRC) has been showing a good performance for face recognition in recent years. But SRC is not good at face recognition with low quality images (e.g., disguised, corrupted, occluded, and so on) which often appear in practical applications. To solve the problem, in this paper, we propose a novel SRC based method for face recognition with low quality images named sparse low-rank component based representation (SLCR). In SLCR, we utilize low-rank matrix recovery on the training dataset to obtain low-rank components and non-low-rank components, which are used to construct the dictionary. The new dictionary is capable of describing facial feature better, especially for low quality face samples. Furthermore, the minimum class-wise reconstruction residual is used as the recognition rule, leading to a substantial improvement on the proposed SLCR's performance. Extensive experiments on benchmark face databases demonstrate that the proposed method is consistently superior to other sparse-representation based approaches for face recognition with low quality images.

Index Terms—Face recognition, sparse-representation based classification, low-rank component, low quality images.

---

1 INTRODUCTION

FACE recognition has been the most popular biometric method due to its huge application potential in the past decades [1], [2], [3], [4], [5], [6], [7], [8]. Sufficient and favourable training samples guarantee a good feature representation for describing the characteristics of an individual's face. However, in the real world, the image of each person is often disguised, corrupted or occluded. Therefore, face recognition with low quality images is more challenging than the one with sufficient and favourable images. This paper focuses on the task of face recognition with low quality images.

The effectiveness of feature extraction is important for face recognition. Principal component analysis (PCA) [9] is a common technique for dimensionality reduction. In addition, there are other methods such as linear discriminant analysis (LDA) [10], probabilistic subspace learning [11] and locality preservation (Laplacianface) [12] and so on. However, it is a difficult task for these methods to solve outliers or sparse noise [13]. To alleviate this problem, some methods on robust PCA have been proposed [14], [15], [16]. Among them, low-rank matrix recovery (LR) [14] is a key technique, which can separate corrupted information from the training face images better than PCA. Accordingly, low-rank components obtained by LR would better serve the classification purpose.

The performance of classifier is important for face recognition. Nearest neighbor (NN) classifier is widely applied for its simplicity. Extensions of NN classifier, nearest feature line (NFL) [17], nearest feature plane (NFP) [18], nearest feature space (NFS) [19] and linear regression classifier (LRC) [20], consider the relation between the testing image and the training images of each class separately [21]. Different from the above-mentioned classifiers, sparse-representation based classification (SRC) which considers the testing image as a linear combination of the training dataset has been proposed for face recognition and achieved satisfying results [22]. However, SRC is incapable of performing well when the training dataset is undersampled or corrupted. To overcome this shortcoming, some extended SRC methods have been proposed [25], [26]. Zhou et al. applied SRC with Markov random fields to address the disguise face recognition problem with large contiguous occlusion [23]. Wagner et al. used SRC to handle the misalignment, pose and illumination invariant recognition problem [24]. Yang et al. borrowed the idea of robust regression [27] and proposed a regularized robust coding (RSC) [28], [29]. He et al. made use of the correntropy induced robust error metric and presented the correntropy based sparse-representation algorithm (CESR) [30], [31]. Lai et al. applied a method of class-wise sparse-representation (CSR) to tackle the problems of the conventional sample-wise sparse-representation [33]. The above methods combining SRC with other techniques improve the classifier's performance, but they still do not resolve low-quality face recognition. Some recent work, on the other hand, began to investigate the dictionary construction in SRC based methods. Deng et al. proposed a superposed sparse-representation-based classifier (SSRC) for undersampled face recognition [32], [34], in which the dictionary simply uses centroid images to capture the face feature. Chen et al. adopted a low-rank matrix approximation algorithm with structural incoherence (LRSI) integrated into SRC for robust face recognition [35]. Jiang et al. proposed a sparse-

- *Shicheng Yang, Le Zhang and Ying Wen are with the Shanghai Key Laboratory of Multidimensional Information Processing, Department of Computer Science and Technology, East China Normal University, Shanghai, China.*
- *Lianghua He is with the Department of Computer Science and Technology, Tongji University, Shanghai, China.*

*Corresponding author: Lianghua He (email: helianghua@tongji.edu.cn) and Ying Wen (email: ywen@cs.ecnu.edu.cn).
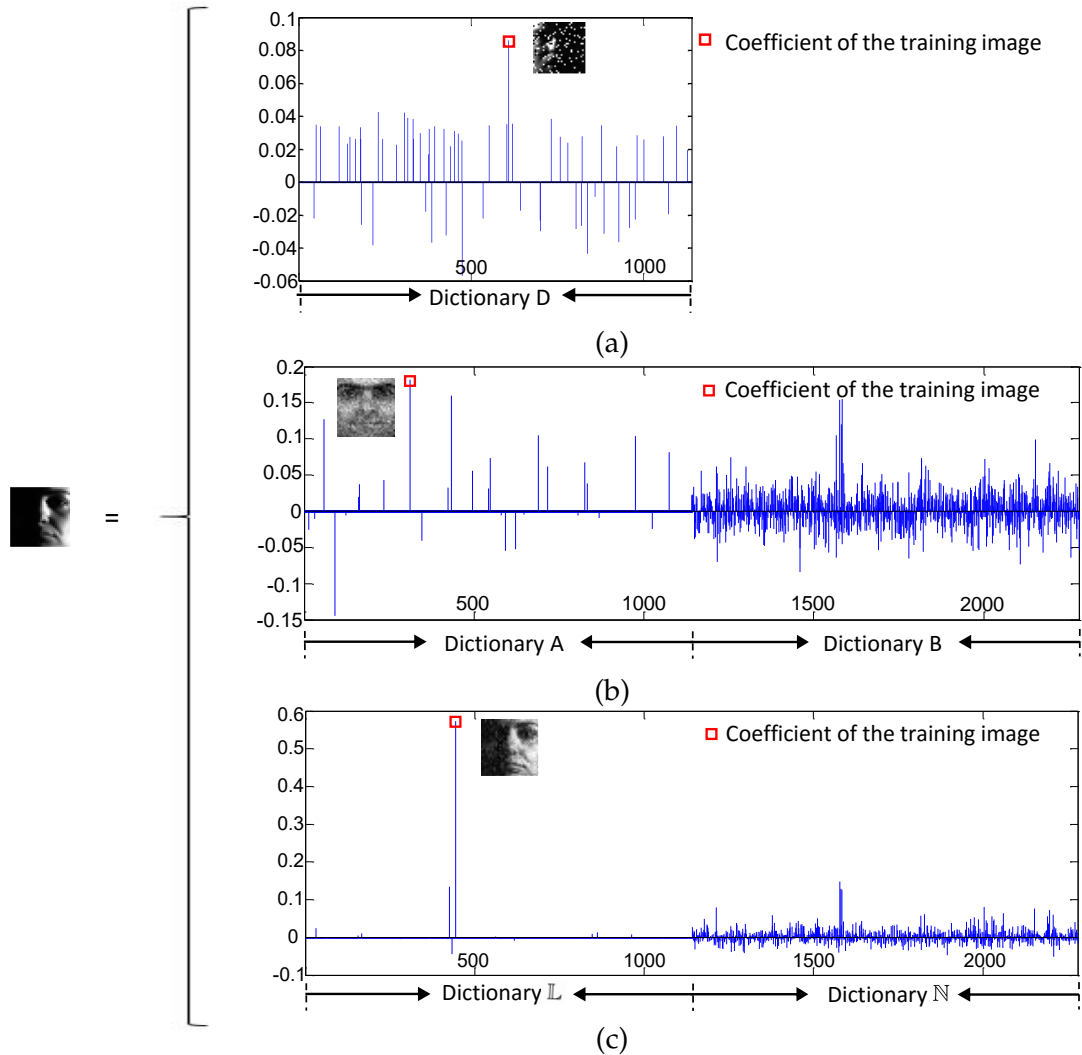
Fig. 1. Recognition with 32×32 training images corrupted by 20% salt-and-pepper noise using (a) SRC, (b) SDR-SLR and (c) SLCR.

and dense-hybrid representation (SDR) [21] by using the reconstructed images by the singular vectors corresponding to the largest singular value to initialize the dictionary. Although the dictionary based SRC methods indeed improve the SRC's performance, to some extent, they still show unsatisfactory results for undersampled, disguised, corrupted and occluded data. This may be because these methods use original samples to construct the dictionary without properly selecting or processing these samples.

In this paper, we focus on the dictionary construction of SRC to solve face recognition with low quality images and propose a sparse low-rank component based representation (SLCR) which is effective for undersampled, disguised, corrupted and occluded face recognition. In the proposed method, the main contribution is the application of the low-rank component decomposition to construct the dictionaries. Low-rank component and non low-rank component obtained by LR from the training samples present the effective features and the others associated with occlusion, outlier or sparse noise, respectively, which would contribute to accurate recognition. Then the Augmented Lagrange Multiplier (ALM) scheme is used to solve the proposed SLCR. Finally,

we minimize class-wise reconstruction residual to recognize the testing image. Furthermore, we analyze the reason why the proposed SLCR can improve face recognition with low quality images in the last section. The experimental results on the extended Yale B, CMU Multi-PIE, AR and LFW databases validate that our method outperforms for face recognition with low quality images.

The remainder of this paper is organized as follows. In Section 2, we present the proposed sparse low-rank component based representation. Experimental results on face image data are reported in Section 3. Finally, Section 4 discusses and concludes this paper.

2 METHOD

This work studies a new sparse low-rank component based representation (SLCR) and its dictionary construction for face recognition with low quality images. Since the proposed method stems from SRC, SSRC and SDR, we introduce these methods briefly.
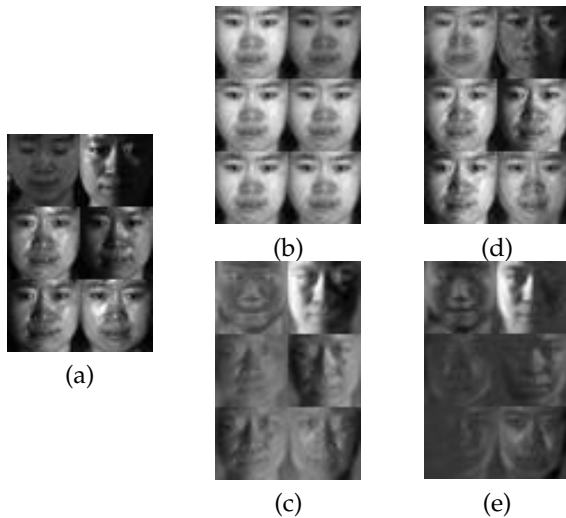
Fig. 2. Dictionary construction. (a) Samples; (b) Class-specific information; (c) non-class-specific information; (d) Low-rank component; (e) non-low-rank component. Note: SRC uses (a); SDR-SLR uses (b+c); SLCR uses (d+e).

2.1 Related Works

Sparse-representation based classification (SRC) algorithm for face recognition considers each testing image as a sparse linear combination of the training images by solving an l_1-minimization problem. Assume that there are N training images from C object classes. Then, define a training dataset $D = [D_1, D_2, ..., D_C] \in R^{d \times N}$, where D_i consists of the training images of ith class as its columns and d is the dimension of each sample. Given a testing image $y \in R^{d \times 1}$, the linear representation of y can be represented in terms of all training images as:

$$y = D\alpha + z \qquad (1)$$

where $\alpha \in R^N$ is a sparse coefficient vector whose entries are zeros except those associated with the ith class and $z \in R^d$ is a reconstruction error term with bounded energy $\|z\|_2 < \varepsilon$. The sparse solution α can be approximately recovered by solving the following stable l_1-minimization problem [22]:

$$\min_{\alpha, z} \|\alpha\|_1 + \beta \|z\|_2^2, \ s.t. \ y = D\alpha + z \qquad (2)$$

where β is a constant for a compromise between sparsity and reconstruction.

SRC is incapable of performing well when the training images are corrupted or undersampled. Therefore, Deng et al. proposed a prototype plus variation (P+V) representation model to improve the robustness against the undersampled and corrupted training images. Then, the linear representation of y can be rewritten in terms of all training images as [32]:

$$y = A\alpha + Bx + z \qquad (3)$$

where A is the prototype dictionary, B is the variation dictionary, α and x can be recovered simultaneously by l_1-minimization. Note that the residual is related to α and x, which is computed as follow:

$$r_i(y) = \left\| y - [A, B] \begin{bmatrix} \delta_i(\alpha) \\ x \end{bmatrix} \right\|_2 \qquad (4)$$

where $\delta_i(\alpha)$ is a new vector whose only nonzero entries are the entries in α that are associated with class i. And then a superposed SRC (SSRC) based on this model is proposed, in which the prototype dictionary A presents the geometric centroid per class and the variation matrix B is composed of the samples based difference to the centroid.

Based on the P+V model, a sparse- and dense-hybrid representation (SDR) framework is proposed, in which dictionary A contains feature information of face images per class namely class-specific component and dictionary B is non-class-specific component. The representation residual in SDR is defined as

$$r_i(y) = \|z - z_i\|_2 = \|A(I - C_i)\alpha\|_2 \qquad (5)$$

where I is an identity matrix, C_i is a class-label matrix of the training dataset D for class i, its element $C_i(k, k) = 1$ if the kth training image originates from class i and all other elements of C_i are zero. To solve the proposed SDR, Jiang et al. proposed a procedure of supervised low-rank dictionary decomposition (SDR-SLR) [21].

2.2 Sparse Low-rank Component based Representation (SLCR)

Motivated by individual strengths of SRC and low-rank matrix recovery, in this paper, we propose a new sparse low-rank component based representation (SLCR) for low quality face recognition. We begin with the motivations of our work.

For the previous dictionary based SRC methods, SSRC simply applies centroid images to capture the class-specific information. SDR-SLR applies the reconstructed images by the singular vectors corresponding to the largest singular value to initialize dictionary. The experiments report that SDR-SLR is superior to SSRC for face recognition [21].

SDR-SLR applies singular value decomposition (SVD) to get class-specific information to initialize the dictionary. For the matrix decomposition, SVD is the same as PCA. By PCA, the training dataset D can be decomposed into

$$D = L + N \qquad (6)$$

where L is the principal component (i.e., class-specific information in SDR-SLR), N is the non-principal component (i.e., non-class-specific information in SDR-SLR). It finds that the best rank-k estimation of L by minimizing $\|D - L\|_2$ subject to $rank(L) <= k$ and it can be solved by SVD. In real application, images are often destroyed by various noise, which may lead to potential error contained in the principal component. If an image is only corrupted by Gaussian noise, the principal component obtained by PCA can be optimal [14]. However, PCA is sensitive to small non-Gaussian noise often appeared in actual face images, which denotes that the information captured by PCA reserves potential errors.

The fact is that face images within a class have a low-rank structure [36]. Thus, the dictionary that only contains class-specific information should be the low-rank matrix. It is obviously hard for SDR-SLR to obtain the optimal low-rank matrix when the training set is corrupted by non-Gaussian noise. However, for whatever noise, we still hope to decompose D into low-rank component $\mathbb{L}$ and non-low-rank component $\mathbb{N}$. Fortunately, low-rank matrix recovery

Fig. 3. The cropped images of one person from the (a) extended Yale B, (b) CMU Multi-PIE and (c) AR database.

can satisfy this demand such that $\mathbb{L}$ can correctly describe the facial feature while $\mathbb{N}$ contains the information associated with sparse error.

By LR, D can be initialized by

$$D = \mathbb{L} + \mathbb{N} \tag{7}$$

where $\mathbb{L}$ is low-rank component from the original training matrix D and $\mathbb{N}$ is non-low-rank component associated with sparse error. This formulation suggests that LR seeks the lowest rank $\mathbb{L}$ that contains almost all of the class-specific information. The lowest rank $\mathbb{L}$ can be approximately recovered by solving the following convex surrogate

$$\min_{\mathbb{L},\mathbb{N}} \|\mathbb{L}\|_* + \gamma \|\mathbb{N}\|_1 , \, s.t. \, D = \mathbb{L} + \mathbb{N} \tag{8}$$

where the nuclear norm $\|\mathbb{L}\|_*$, the sum of the singular values, approximates the rank of $\mathbb{L}$ and γ is a constant for a compromise between $\mathbb{L}$ and $\mathbb{N}$. Then, we use $\mathbb{L}$ and $\mathbb{N}$ to construct the dictionary.

Then, the testing image y can be rewritten as

$$y = \mathbb{L}\alpha + \mathbb{N}x + z \tag{9}$$

where z is the reconstruction error. Eq.(9) is the proposed sparse low-rank component based representation (SLCR). The sparsity of α is measured by l_0-norm of α. But this problem is NP-hard, we replace l_0-norm of α by l_1-norm of α, i.e. $\|\alpha\|_1$. In order to make the reconstruction error z as small as possible, it is unnecessary to put the sparse constraint on x and therefore we use $\|x\|_2$. The solution of the proposed SLCR, α, x and z, is obtained by solving the following optimization problem:

$$\min_{\alpha,x,z} \|\alpha\|_1 + \beta \|x\|_2^2 + \gamma \|z\|_1 , \, s.t. \, y = \mathbb{L}\alpha + \mathbb{N}x + z \tag{10}$$

where β and γ are constants for a compromise. We use the Augmented Lagrange Multiplier (ALM) scheme [37] to solve the optimization problem. Finally, our recognition rule is also based on minimum class-wise reconstruction residual. The class-wise reconstruction residual is defined by

$$r_i(y) = \|z - z_i\|_2 = \|\mathbb{L}(I - C_i)\alpha\|_2 \tag{11}$$

where $\mathbb{L}$ is the low-rank dictionary of SLCR.

Next, we carry out an experiment to show the difference among SRC, SDR-SLR and SLCR. We randomly select 30 images corrupted by 20% salt-and-pepper noise from the extended Yale B database [38] as a training set and randomly select a testing image to get the results of SRC, SDR-SLR and SLCR. Figs. 1 (a), (b) and (c) present the sparse coefficients

of a testing image using SRC, SDR-SLR and SLCR, respectively. It is noted that sparse coefficients obtained by SLCR are sparser than those of SRC and SDR-SLR. The training samples of the correct subject contains the noise, which results in SRC and SDR-SLR selecting the samples of many other subjects to represent the testing image. Thus, the most significant coefficients of SRC and SDR-SLR associated with wrong subjects lead to misclassification in this example. Contrary to SRC and SDR-SLR, the top significant coefficient of SLCR is for the training image of the same identity as the testing image. This denotes SLCR obtains a correct result in such a situation. From this example, we can see that the proposed SLCR method obtains more sparse and accurate coefficients.

The difference among SRC, SDR-SLR and SLCR mainly is reflected in the dictionary construction. Fig. 2 shows an example of the dictionary construction of the proposed SLCR comparing to SRC and SDR-SLR on the CMU Multi-PIE database [39]. Fig. 2 (a) shows the dictionary of SRC constructed by all original images. As we can see, the dictionary in SRC includes all samples without class-specific information. Fig. 2 (b) and Fig. 2 (c) are class-specific images and non-class specific images, both of which are the initial dictionary of SDR-SLR. Fig. 2 (d) and Fig. 2 (e) are low-rank component and non-low-rank component, both of which construct the dictionary of SLCR. Generally, a good dictionary not only can well describe facial feature, but also can reduce the impact of sparse error. Thus, we want to propose a new dictionary which may be more suitable for the recognition and effectively reduce the error. Because of low-rank structure existing in face images within a class [36], low-rank component can describe facial feature well. Hence, the dictionary constructed by low-rank component can satisfy our purpose. In the following experiments, we will testify of the performance of the proposed SLCR.

3 EXPERIMENTS

We propose a sparse low-rank component based representation (SLCR) which is an extension of sparse-representation based classification (SRC). Thus, we compare the results between SLCR and other SRC based methods. In this section, we first choose three face databases (the extended Yale B [38], CMU Multi-PIE [39] and AR [40] face databases) to compare the performance of our method with LR, SRC, LRSI, SSRC and SDR-SLR in different experimental circumstances. Furthermore, we verify the performance of SLCR and other SRC based methods on LFW database [41] in natural situations. All images are cropped with size 32×32. In addition, all experiments are repeated 10 times and each time we choose different training set and testing set. Training set and testing set are from the same database. Both of them contain different samples of the same person. Thus, the number of impostor samples in the training set and testing set is 0 so that the false match rate (FMR) is 0% in all experiments. We use the false non-match rate (FNMR) at a 0% FMR to show the results of experiments.

3.1 Experiments on Face Database

The extended Yale B database consists of 2414 frontal-face images of 38 subjects (around 59-64 images per per-

TABLE 1
Experimental results on the CMU Multi-PIE database (reported as %FNMR@FMR=0%).

Train.number	2	3	4	5	6
LR	34.34 ±1.13	26.42 ±1.52	20.55 ±1.64	16.28 ±1.63	12.57 ±0.81
SRC	66.14 ±3.23	32.42 ±1.53	18.50 ±1.74	11.53 ±0.89	8.33 ±0.60
LRSI	31.87 ±1.08	23.31 ±1.06	18.04 ±1.13	14.37 ±1.52	11.91 ±0.88
SSRC	21.54 ±1.39	12.32 ±0.93	9.19 ±0.79	8.11 ±0.61	7.28 ±0.70
SDR-SLR	22.31 ±1.37	13.20 ±1.21	9.30 ±1.38	6.77 ±1.02	5.33 ±0.59
SLCR	**18.58** ±**2.34**	**12.07** ±**0.76**	**9.17** ±**0.81**	**6.17** ±**0.66**	**5.00** ±**0.43**

TABLE 2
Experimental results on the extended Yale B database (reported as %FNMR@FMR=0%).

Train.number	2	3	4	5	6
LR	60.80 ±2.00	48.79 ±1.77	42.58 ±1.92	37.75 ±1.08	33.06 ±0.66
SRC	79.49 ±1.69	58.63 ±1.27	43.12 ±1.67	33.59 ±1.13	26.63 ±0.97
LRSI	59.22 ±2.51	47.37 ±1.82	40.85 ±1.99	36.34 ±1.45	31.87 ±0.53
SSRC	51.06 ±2.96	36.79 ±2.02	28.63 ±1.62	22.57 ±0.58	18.04 ±1.21
SDR-SLR	54.79 ±3.67	41.50 ±2.55	33.70 ±2.29	27.79 ±1.81	22.58 ±1.83
SLCR	52.20 ±2.92	40.37 ±2.55	33.40 ±1.82	26.85 ±1.05	21.48 ±1.78

Fig. 4. Experimental results on images with sunglasses on the AR database. Reported is the FNMR at a 0% FMR.
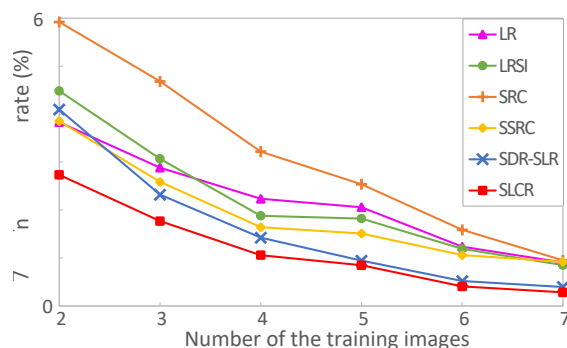
Fig. 5. Experimental results on images with scarf on the AR database. Reported is the FNMR at a 0% FMR.

son), while each image is taken under various laboratory-controlled lighting conditions. The CMU Multi-PIE database contains face images captured in four sessions with variations in illumination, expression and pose. And we choose a subset of the dataset set consisting of 1360 frontal images for 68 individuals. The AR database contains over 4000 frontal images for 126 individuals. We choose a subset of the dataset set consisting of 702 frontal images for 54 individuals on AR database and these images include more facial variations, including illumination change, expressions, and facial disguises. The cropped images of one person from the extended Yale B, CMU Multi-PIE and AR databases are shown in Fig. 3 (a), (b) and (c), respectively.

We conduct four groups of experiments to validate the proposed method performance.

- Undersampled training dataset on the Yale B and PIE databases.
- Real disguised (scarf or glasses disguise) images in both training and testing data on the AR database.
- Training dataset corrupted by different levels of salt and pepper noise.
- Training dataset occluded by various sizes of contiguous block image.

The purpose of this paper is to solve face recognition with low-quality images, thus the last three groups work on the low-quality images with disguised, corrupted and occluded subjects. The first group's purpose is to validate the proposed method for undersampled face recognition, which is also an issue in the current face recognition.

3.1.1 Experiments on Undersampled Training Dataset

This subsection tests the effectiveness of various approaches on the undersampled training dataset.

Firstly, we carry out this experiment on CMU Multi-PIE face database. We randomly select 2 - 6 images per individual as the training set and the rest of the images as the testing set. The average false non-match rates and the standard deviations of 10 runs are shown in Table 1. Although undersampled training dataset does not have sufficient representative samples to describe facial feature, SLCR is better than the other methods for the undersampled problem. This is because SLCR uses low-rank component which contains important facial feature to construct the dictionary.

Then, we randomly select 2 - 6 images per individual on the extended Yale B database as the training set and the rest images as the testing images. The average false non-match rates and standard deviations of 10 runs are showed in Table 2. It is generally known that SSRC simply uses centroid images to capture the feature information. In the extended Yale B database, face images of one person have little pose and emotion changes while the greatest change is illumination, as is shown in Fig. 3 (a). Thus, the feature information captured by centroid images is able to adapt to the extended Yale B database and SSRC presents a good result. However, other databases such as AR and CMU Multi-PIE give emphasis to other changes, thus SSRC cannot do better than other methods. The SLCR method is slightly weaker than SSRC but superior to SDR-SLR, LR and LRSI on the
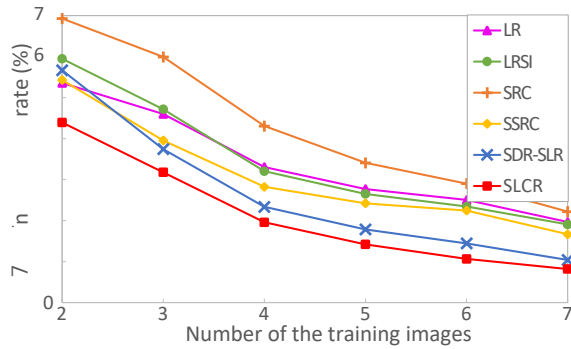
Fig. 6. Experimental results on images with sunglasses or scarf on the AR database. Reported is the FNMR at a 0% FMR.

5%   10%   15%   20%   25%   30%
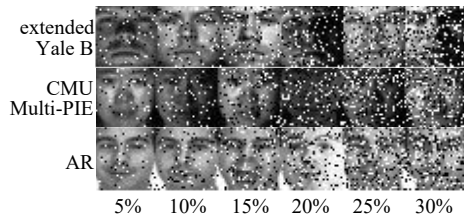
Fig. 7. Some training images corrupted by salt-and-pepper noise. From top to bottom, the training images are from the extended Yale B, CMU Multi-PIE and AR databases, respectively. From left to right, the training images are corrupted by salt-and-pepper noise from 5% to 30%, respectively.

extended Yale B database. The above experiments show that SLCR is comparable to other methods for undersampled face recognition.

3.1.2 Experiments on Real Disguised Images

This subsection tests the effectiveness of various approaches with real images of disguised subjects in both training and testing images. We choose AR dataset to testify of the performance of SLCR.

We randomly choose 2 - 6 images per individual with sunglasses or scarf and some neutral images as the training set and the remaining images are as the testing set, in which the training images have mixed types of variations. Firstly, we randomly choose some sunglasses and neutral images as the training set. The average false non-match rates of 10 runs are plotted in Fig. 4. It can be seen that SLCR consistently outperforms SDR-SLR, SSRC, LR and LRSI when the training images is undersampled and disguised. Secondly, we randomly choose some scarf and neutral images as the training set. The results are plotted in Fig. 5. Similar to the previous experiment, SLCR achieves a good performance for undersampled and disguised data. Lastly, to further verify the performance of SLCR, we randomly choose some sunglasses, scarf and neutral image as the training set. The average false non-match rates are shown in Fig. 6. With the increase of the training samples, the superiority of SLCR is obvious and SLCR presents a good performance for the sunglasses or scarf disguised images. For face recognition in the disguised data, the proposed method is optimal. This is because the dictionary in SLCR composed of low-rank component and non-low-rank component is able to describe the facial feature better, especially for real disguised (scarf

or sunglasses disguise) face images, meanwhile the scarf and sunglasses disguise may adverse effects on the other methods.

The above experiments show that SLCR method is robust to illumination, appearance, and make up for face recognition. In addition, it is also verified that SLCR is superior to the other methods when the number of the training images per class is insufficient.

3.1.3 Experiments on Images Corrupted by Noise
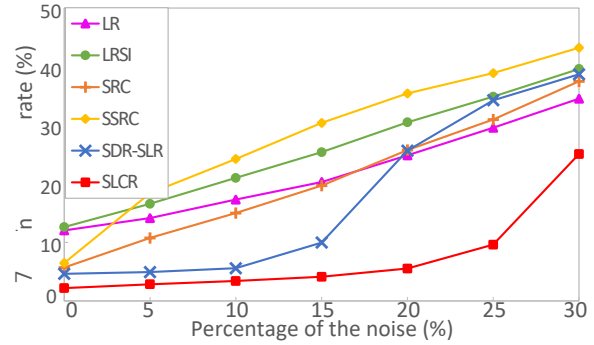
Fig. 8. Experimental results on 20 corrupted training images on the extended Yale B database. Reported is the FNMR at a 0% FMR.
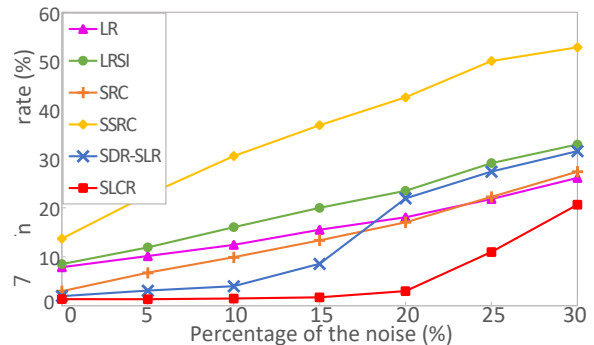
Fig. 9. Experimental results on 30 corrupted training images on the extended Yale B database. Reported is the FNMR at a 0% FMR.
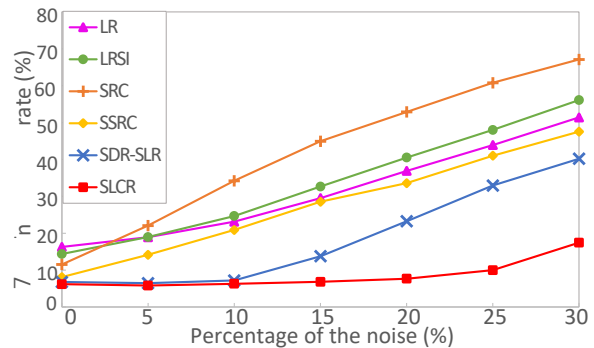
Fig. 10. Experimental results on 5 corrupted training images on the CMU Multi-PIE database. Reported is the FNMR at a 0% FMR.

The experiment aims to test the effectiveness of the proposed SLCR on the training dataset corrupted by different levels of noise.
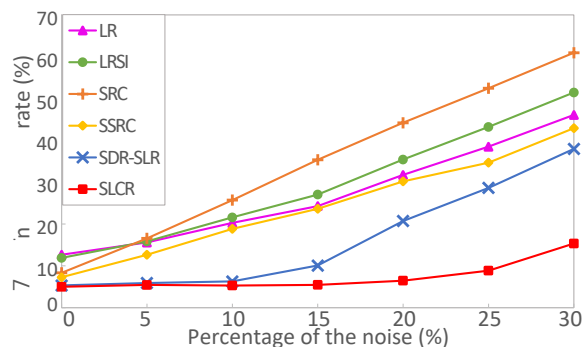
Fig. 11. Experimental results on 6 corrupted training images on the CMU Multi-PIE database. Reported is the FNMR at a 0% FMR.
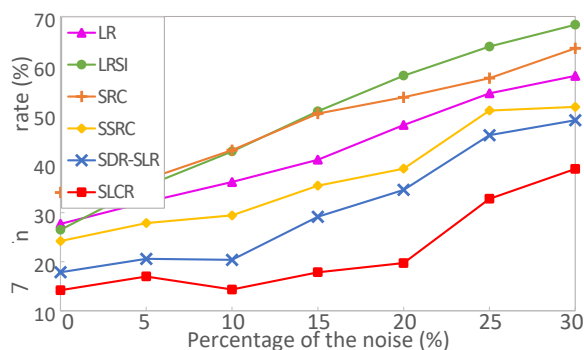
Fig. 12. Experimental results on 5 corrupted training images on the AR database. Reported is the FNMR at a 0% FMR.

We select the extended Yale B, CMU Multi-PIE and AR databases to test and all training samples are corrupted by different levels of noise. As shown in Fig. 7, from top to bottom, the training images are from the extended Yale B, CMU Multi-PIE and AR databases respectively, and from left to right, the training images are corrupted by salt-and-pepper noise from 5% to 30%, respectively. Considering different databases having different sample size, we randomly choose 20 and 30 images per individual from the extended Yale B database, 5 and 6 images per individual from PIE and AR databases as the training set and the rest as the testing set, respectively. Figs. 8-13 plot the average false non-match rates of different training set in different databases,
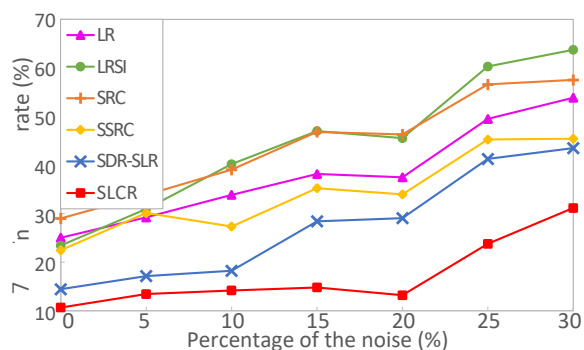
Fig. 13. Experimental results on 6 corrupted training images on the AR database. Reported is the FNMR at a 0% FMR.

TABLE 3
Experimental results with 20 occluded training images on the extended Yale B database (reported as %FNMR@FMR=0%).

Percent corrupted	10%	15%	20%	25%	30%	35%	40%
LR	18.55 ±1.15	21.89 ±1.41	26.17 ±1.37	33.17 ±1.16	37.38 ±1.59	41.09 ±1.96	47.91 ±2.41
SRC	9.00 ±0.55	10.99 ±0.88	13.88 ±0.87	16.88 ±1.11	19.31 ±0.99	21.53 ±1.21	28.49 ±1.39
LRSI	19.29 ±0.77	22.29 ±1.19	26.83 ±1.38	32.38 ±0.80	36.71 ±1.77	40.17 ±1.50	46.90 ±1.55
SSRC	10.67 ±0.71	12.13 ±0.97	14.16 ±0.77	18.63 ±0.99	22.56 ±1.58	29.89 ±1.24	26.86 ±2.67
SDR-SLR	8.01 ±0.91	9.00 ±0.81	10.40 ±1.14	11.88 ±0.69	12.49 ±1.72	13.89 ±0.74	16.78 ±1.03
SLCR	**5.37 ±0.59**	**6.03 ±0.81**	**6.35 ±0.47**	**7.27 ±1.15**	**7.85 ±1.03**	**8.35 ±0.96**	**10.28 ±0.95**

respectively. From these figures, the performances of the aforementioned methods decline with increasing level of noise. SSRC uses the centroid images to construct the dictionary which contain the noise. Thus, the noise in the training images may impact the performance of SSRC. Similarly, the dictionary in SDR-SLR also comprises the information associated noise, thus SDR-SLR cannot achieve good results. Because of the dictionary constructed by low-rank component from the corrupted training images in SLCR, the dictionary contains more class specific information. Thus, SLCR has better performance than the others. Furthermore, the superiority of SLCR is obvious particularly when the level of noise is more than 10%. It means that SLCR is accurate, reliable and with good repeatability.

The above experiments show that the performance of SLCR is superior to LR, LRSI, SRC, SSRC and SDR-SLR, and also demonstrate that SLCR is more robust than the other methods for the training dataset corrupted by noise.

3.1.4 Experiments on the Images Occluded by Block Image
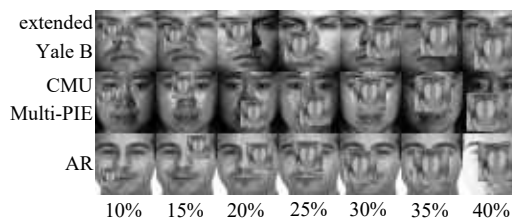
Fig. 14. Some training images occluded by block image. From top to bottom, the training images are from the extended Yale B, CMU Multi-PIE and AR databases, respectively. From left to right, the training images are occluded from 10% to 40%, respectively.

The experiment is to test the effectiveness of different approaches on the training dataset occluded by various sizes of contiguous square block image.

Similar to the previous experiments, we also choose the above databases to test the robustness of the proposed method. The images in the training set are occluded by replacing a randomly located square block image. The design of the experimental data is shown in Fig. 14, in which from top to bottom the training images are from the extended Yale B, CMU Multi-PIE and AR databases respectively, and from left to right 10, 15, 20, 25, 30, 35 and 40 percent of images are occluded respectively. 20 and 30 images per individual from extended Yale B database, 5 and 6 images

TABLE 4
Experimental results with 30 occluded training images on the extended Yale B database (reported as %FNMR@FMR=0%).

Percent corrupted	10%	15%	20%	25%	30%	35%	40%
LR	14.21 ±0.80	16.73 ±1.18	21.78 ±1.35	27.06 ±1.26	32.31 ±1.93	39.96 ±0.93	45.02 ±2.25
SRC	5.82 ±0.73	7.36 ±0.69	9.57 ±0.78	12.55 ±0.69	14.25 ±0.72	20.35 ±0.83	24.01 ±0.82
LRSI	15.31 ±0.76	17.14 ±1.34	21.81 ±1.23	27.05 ±0.90	30.35 ±1.55	36.15 ±1.08	40.93 ±2.07
SSRC	19.22 ±1.36	21.44 ±1.29	24.61 ±1.37	30.29 ±0.96	38.29 ±1.29	78.67 ±2.61	94.23 ±0.67
SDR-SLR	5.25 ±0.79	6.14 ±0.69	6.91 ±0.63	8.28 ±0.70	9.09 ±1.45	10.96 ±1.08	11.73 ±0.90
SLCR	**3.06** ±0.48	**3.19** ±0.44	**3.56** ±0.39	**3.81** ±0.28	**4.39** ±0.48	**5.42** ±0.63	**7.06** ±0.68

TABLE 6
Experimental results with 6 occluded training images on the CMU Multi-PIE database (reported as %FNMR@FMR=0%).

Percent corrupted	10%	15%	20%	25%	30%	35%	40%
LR	19.57 ±1.60	23.21 ±2.32	28.21 ±1.56	34.25 ±1.82	38.64 ±1.75	43.91 ±2.80	45.95 ±2.00
SRC	15.13 ±1.76	18.31 ±1.85	21.40 ±1.50	25.74 ±1.25	28.45 ±1.29	32.70 ±1.58	36.12 ±1.32
LRSI	17.79 ±1.51	21.58 ±1.87	25.39 ±1.24	29.65 ±2.01	33.78 ±1.95	38.81 ±1.95	38.85 ±1.80
SSRC	9.11 ±0.89	8.95 ±0.84	10.18 ±0.89	11.32 ±0.69	12.32 ±0.50	17.45 ±1.12	23.93 ±2.49
SDR-SLR	6.81 ±0.77	7.14 ±0.86	8.03 ±1.09	8.72 ±0.65	8.76 ±0.93	9.76 ±0.96	11.01 ±1.22
SLCR	**6.26** ±0.78	**6.76** ±0.73	**7.52** ±1.09	**7.98** ±0.61	**8.08** ±0.56	**9.22** ±1.01	**9.75** ±0.87

TABLE 5
Experimental results with 5 occluded training images on the CMU Multi-PIE database (reported as %FNMR@FMR=0%).

Percent corrupted	10%	15%	20%	25%	30%	35%	40%
LR	22.16 ±1.24	26.89 ±1.26	31.36 ±1.51	38.13 ±2.78	42.59 ±1.91	45.19 ±1.78	51.07 ±2.63
SRC	21.01 ±1.38	24.29 ±1.07	27.96 ±1.66	33.30 ±1.85	35.84 ±1.96	39.20 ±1.43	44.81 ±1.68
LRSI	20.25 ±0.79	24.21 ±1.18	27.71 ±1.35	33.57 ±2.83	36.90 ±2.43	39.83 ±2.33	44.23 ±3.03
SSRC	10.15 ±0.60	10.46 ±1.00	10.60 ±0.89	12.87 ±1.64	13.99 ±1.68	15.66 ±1.44	23.55 ±2.69
SDR-SLR	8.15 ±0.61	8.95 ±1.07	9.26 ±0.61	10.4 ±1.61	11.35 ±1.34	11.55 ±0.98	13.48 ±1.34
SLCR	**7.64** ±0.44	**8.49** ±1.00	**8.61** ±0.84	**10.08** ±1.73	**10.87** ±1.53	**11.22** ±0.72	**12.65** ±1.22

TABLE 7
Experimental results with 5 occluded training images on the AR database (reported as %FNMR@FMR=0%).

Percent corrupted	10%	15%	20%	25%	30%	35%	40%
LR	40.32 ±8.47	43.13 ±11.39	46.32 ±7.00	48.24 ±5.15	52.69 ±8.00	52.48 ±8.26	54.14 ±4.45
SRC	44.81 ±7.08	48.01 ±10.34	50.88 ±7.49	51.94 ±4.45	54.68 ±7.42	56.74 ±7.59	56.35 ±4.84
LRSI	37.69 ±7.76	42.96 ±9.72	44.35 ±7.30	49.51 ±3.55	50.93 ±6.68	52.78 ±7.06	53.96 ±2.36
SSRC	30.88 ±7.83	34.42 ±9.96	35.25 ±8.12	36.11 ±6.70	39.91 ±8.62	42.13 ±6.98	44.77 ±5.83
SDR-SLR	24.98 ±7.41	27.73 ±10.92	28.38 ±8.83	31.78 ±5.53	33.91 ±9.60	34.44 ±9.71	32.94 ±6.70
SLCR	**23.22** ±7.62	**25.07** ±9.63	**27.36** ±7.95	**29.12** ±6.69	**32.25** ±10.27	**32.59** ±9.21	**31.11** ±6.02

per individual from PIE and AR databases are chosen as the training set and all rest images are used as the testing set, respectively. The average false non-match rates and standard deviations of 10 runs of three groups of experiments are shown in Tables 3-8, respectively. From these tables, we can see that SLCR still has better performance than the other methods. SSRC is almost the worst method among these methods. SSRC uses the centroid images to capture the class-specific information and the centroid images may contain the block occlusion that impacts recognition performance. The dictionary in SDR-SLR also contains the block occlusion, thus it cannot obtain the best result. Thanks to its low-rank recovery of the training dataset, the result of SLCR is more approximate to the practical result than that of the other methods. For example, in Table 4, we can see the accuracy of SDR-SLR (10.96%) over the proposed SLCR (5.42%) reaches about 5.54% at 30 training samples with 35% images occluded. Generally speaking, SLCR achieves better results than other methods for all levels of block occlusion.

The above experiments show that the performance of SLCR is the best and the most robust for the training dataset occluded by block image.

3.2 Experiments on Labeled Face Images in the Wild

The LFW face database [41] is designed for studying the problem of unconstrained face recognition which contains more than 13,000 images of faces collected from the web. Each face has been labeled with the name of the person pictured. Here we adopt a subset of LFW deep funneled images [42] to test the performance of the proposed method. We simply crop the face image to remove the background. In our experiment, we choose 8 face images from each subject and in total 94 subjects are chosen. Some cropped images from the LFW database are shown in Fig. 15. We randomly select 3 - 6 images per individual as the training set and the rest images as the testing set. Table 9 summarizes the false non-match rates on the LFW database. From this table, SLCR clearly outperforms other SRC based approaches when different training size is considered. In the following experiments, we consider more challenging databases which contain not only face images with realistic variations, but also the corrupted and occluded ones for recognition.

As in the previous subsection, we randomly choose 5 and 6 images per individual as the training set and the rest

Fig. 15. Some cropped images from LFW database.

TABLE 8
Experimental results with 6 occluded training images on the AR database (reported as %FNMR@FMR=0%).

Percent corrupted	10%	15%	20%	25%	30%	35%	40%
LR	28.68 ±5.19	29.89 ±5.94	35.90 ±5.91	41.88 ±7.13	44.37 ±7.14	49.68 ±6.94	51.22 ±3.71
SRC	32.70 ±4.06	32.86 ±6.21	38.17 ±3.73	51.14 ±6.64	53.63 ±6.21	51.14 ±8.76	50.74 ±5.22
LRSI	28.23 ±5.70	28.99 ±4.76	37.80 ±5.94	41.75 ±6.27	43.97 ±6.84	48.10 ±6.74	50.61 ±2.79
SSRC	22.70 ±3.86	22.46 ±5.20	25.32 ±7.47	28.52 ±6.88	32.38 ±9.03	40.11 ±7.41	42.67 ±5.64
SDR-SLR	11.75 ±3.43	13.39 ±7.41	16.48 ±6.08	20.50 ±8.70	23.36 ±8.76	28.41 ±8.97	27.65 ±6.59
SLCR	**10.77 ±3.32**	**11.59 ±6.93**	**15.40 ±5.68**	**18.73 ±8.57**	**20.21 ±9.58**	**26.93 ±8.72**	**27.40 ±6.79**

TABLE 9
Experimental results on the LFW database (reported as %FNMR@FMR=0%).

Train.number	3	4	5	6
LR	64.87 ±1.37	63.16 ±1.75	57.98 ±2.11	55.48 ±1.83
SRC	78.87 ±1.08	71.25 ±1.26	65.14 ±2.67	59.68 ±3.26
LRSI	71.60 ±1.49	64.68 ±1.08	60.50 ±2.03	55.00 ±2.41
SSRC	60.19 ±2.24	55.37 ±2.18	53.83 ±2.67	54.04 ±3.33
SDR-SLR	40.21 ±1.01	34.31 ±2.12	27.66 ±2.52	22.34 ±2.23
SLCR	39.57 ±0.93	29.47 ±2.54	24.89 ±1.05	20.21 ±1.78

as the testing set on LFW database. All training samples are corrupted by different levels of noise. Figs. 16-17 plot the 10 runs' average false non-match rates of different training set in different levels of noise, respectively. It can be seen that, since SLCR requires a low-rank dictionary for handling corrupted testing inputs, it is able to achieve satisfactory performance. SLCR consistently outperforms other SRC based methods especially when the level of noise is more than 10%. To some extent, the superiority of SLCR is obvious gradually with the increase of noise. Next, the images of training set are occluded by replacing a randomly located square block image. Tables 10-11 list and compare the average false non-match rates of 10 runs, respectively. From these tables, we see that SLCR is able to achieve comparable results while the performances of other SRC based methods degrade.

The above experiments show that the performance of SLCR is robust for realistic low quality face database.

4 DISCUSSION AND CONCLUSION

Our proposed SLCR consistently outperforms other sparse-representation based methods for face recognition with low quality images. Hence, we analyze the reason why the proposed SLCR can fairly well solve the recognition problem of low quality face images. We choose an example in noise experiments (i.e., Subsection 3.3) to illustrate the procedure of the above experiments. The training samples corrupted by noise and the dictionaries reconstructed by three methods on the CMU Multi-PIE database are compared in Fig. 18. We randomly select 6 face images of the same person to reconstruct faces and extract noises. Fig 18
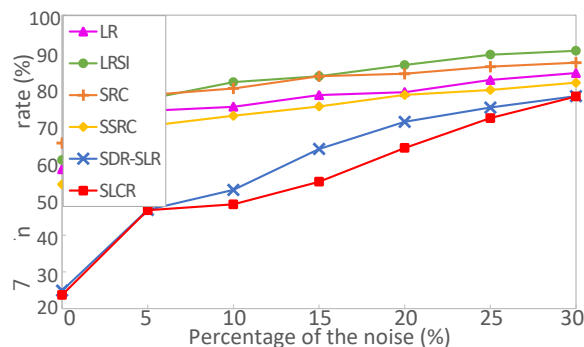
Fig. 16. Experimental results on 5 corrupted training images on the LFW database. Reported is the FNMR at a 0% FMR.
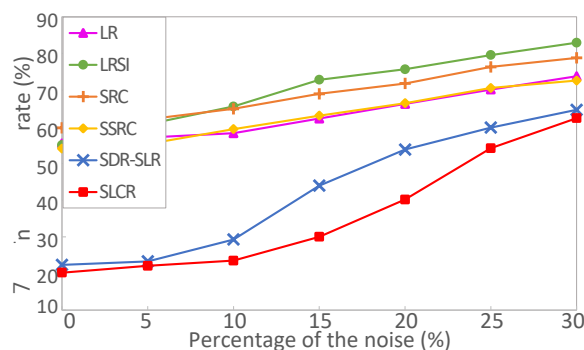
Fig. 17. Experimental results on 6 corrupted training images on the LFW database. Reported is the FNMR at a 0% FMR.

(a) shows 6 face images corrupted by 20% salt-and-pepper noise, which is the dictionary of SRC exactly. Figs. 18 (b) and (c) make up the reconstructed dictionary which simply uses centroid images to capture the class specific information in SSRC. The reconstructed dictionary by the singular vectors corresponding to the largest singular value in SDR-SLR is
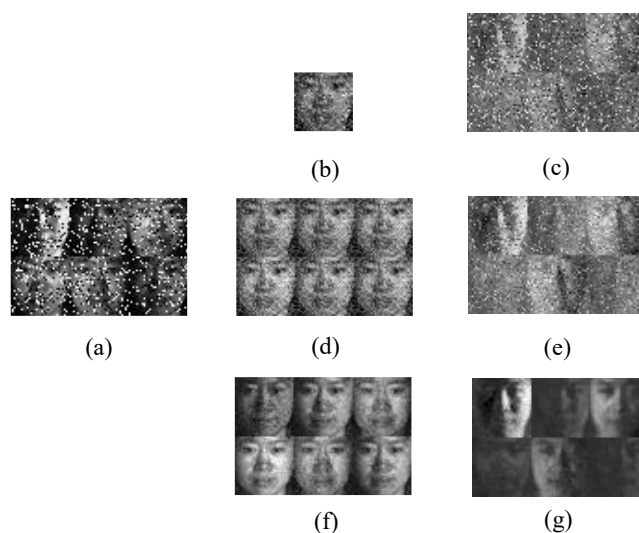
Fig. 18. The corrupted faces and the reconstructed dictionaries by three methods. Note: (a) is the corrupted face; (b) and (c) are from SSRC; (d) and (e) are from SDR-SLR; (f) and (g) are from SLCR.

TABLE 10
Experimental results with 5 occluded training images on the LFW
database (reported as %FNMR@FMR=0%).

Percent corrupted	10%	15%	20%	25%	30%	35%	40%
LR	63.26 ±2.19	65.60 ±1.20	69.72 ±1.80	73.90 ±1.05	76.91 ±2.28	77.87 ±2.33	81.35 ±0.89
SRC	70.28 ±1.74	71.38 ±1.53	74.29 ±2.65	77.12 ±2.69	78.84 ±2.12	80.67 ±1.65	84.22 ±1.49
LRSI	66.03 ±2.18	68.01 ±2.15	73.55 ±1.45	75.39 ±1.90	77.87 ±1.02	78.80 ±1.98	81.91 ±1.06
SSRC	63.83 ±2.87	66.74 ±1.80	71.28 ±3.69	73.76 ±2.07	74.89 ±3.02	75.80 ±1.96	79.89 ±2.97
SDR-SLR	36.45 ±0.68	40.22 ±1.39	48.16 ±3.15	52.48 ±1.97	57.87 ±2.77	60.07 ±2.28	66.81 ±3.39
SLCR	**34.68 ±1.10**	**38.73 ±0.51**	**46.24 ±3.18**	**49.35 ±2.00**	**56.10 ±2.68**	**58.52 ±1.57**	**62.81 ±3.39**

TABLE 11
Experimental results with 6 occluded training images on the LFW
database (reported as %FNMR@FMR=0%).

Percent corrupted	10%	15%	20%	25%	30%	35%	40%
LR	64.26 ±2.21	68.01 ±2.15	67.98 ±3.09	72.23 ±1.12	74.82 ±1.71	76.81 ±1.34	79.15 ±2.11
SRC	65.74 ±3.36	68.72 ±2.39	70.74 ±2.13	72.93 ±2.84	77.50 ±2.77	78.50 ±2.76	80.74 ±2.43
LRSI	64.89 ±3.94	64.57 ±1.58	69.36 ±1.98	74.47 ±2.49	75.85 ±2.78	76.81 ±3.18	79.57 ±3.07
SSRC	65.32 ±3.43	67.34 ±3.79	68.09 ±2.94	72.23 ±3.50	75.96 ±3.46	76.60 ±2.67	82.98 ±2.31
SDR-SLR	35.11 ±3.34	37.77 ±2.44	43.62 ±2.17	49.89 ±3.12	54.47 ±2.57	56.81 ±3.54	63.83 ±3.19
SLCR	**32.98 ±1.71**	**36.17 ±2.69**	**41.49 ±2.08**	**47.61 ±3.12**	**50.80 ±2.55**	**52.13 ±3.69**	**59.31 ±3.41**

depicted in Figs. 18(d) and (e). Similarly, Figs. 18 (f) and (g) are the reconstructed dictionary by SLCR which contains low-rank and non-low-rank component. We can see that SRC, SSRC, as well as SDR-SLR, are unable to effectively remove the noises in faces, i.e., there exists much noise in the dictionary of the three methods. On the contrary, SLCR uses low-rank matrix recovery to get low-rank component and non-low rank component which have less noise in all face images. In other words, the dictionary in SLCR not only can describe facial features well, but also can reduce the impact of noises. The better noise fitting capability of SLCR thus leads to better face recognition performance. The process of dictionary construction in SLCR can remove lots of information caused by noises. At the same time, the dictionary in SLCR maintains more diversity than the other methods. Thus, SLCR achieves robust performance in these experiments. For the other databases and other low quality images (i.e., disguised and occluded), the situation is similar.

In this paper, we proposed a sparse low-rank component based representation for face recognition with low quality images. This work alleviates the impact of low quality training dataset for face recognition. We use the ALM scheme to obtain the solution of the proposed SLCR. Then we recognize a testing image by minimizing class-wise reconstruction residual. Thus, SLCR achieves better classification performance. The experiments show that SLCR is superior to the other SRC based methods for face recognition with low quality images, especially for disguised, corrupted and occluded data.

REFERENCES

[1] T. Larrain, J. S. Bernhard, D. Mery, and K. W. Bowyer, "Face recognition using sparse fingerprint classification algorithm," *IEEE Transactions on Information Forensics and Security*, vol. 12, no. 7, pp. 1646–1657, 2017.

[2] J. Lu, J. Hu, and Y. Tan, "Discriminative deep metric learning for face and kinship verification," *IEEE Transactions on Image Processing*, vol. 26, no. 9, pp. 4269–4282, 2017.

[3] Y. Wen, K. Zhang, Z. Li, and Y. Qiao, "A discriminative feature learning approach for deep face recognition," in *European Conference on Computer Vision*. Springer, 2016, pp. 499–515.

[4] C. Wei and Y. F. Wang, "Undersampled face recognition via robust auxiliary dictionary learning," *IEEE Transactions on Image Processing*, vol. 24, no. 6, pp. 1722–1734, 2015.

[5] G. Goswami, M. Vatsa, and R. Singh, "Face verification via learned representation on feature-rich video frames," *IEEE Transactions on Information Forensics and Security*, vol. 12, no. 7, pp. 1686–1698, 2017.

[6] C. Peng, X. Gao, N. Wang, and J. Li, "Graphical representation for heterogeneous face recognition," *IEEE transactions on pattern analysis and machine intelligence*, vol. 39, no. 2, pp. 301–312, 2017.

[7] N. Werghi, C. Tortorici, S. Berretti, and A. Del Bimbo, "Boosting 3d lbp-based face recognition by fusing shape and texture descriptors on the mesh," *IEEE Transactions on Information Forensics and Security*, vol. 11, no. 5, pp. 964–979, 2016.

[8] H. Roy and D. Bhattacharjee, "Local-gravity-face (lg-face) for illumination-invariant and heterogeneous face recognition," *IEEE Transactions on Information Forensics and Security*, vol. 11, no. 7, pp. 1412–1424, 2016.

[9] M. Turk and A. Pentland, "Eigenfaces for recognition," *Journal of Cognitive Neuroscience*, vol. 3, no. 1, pp. 71–86, 1991.

[10] P. N. Belhumeur, J. P. Hespanha, and David J. Kriegman, "Eigenfaces vs. fisherfaces: Recognition using class specific linear projection," *IEEE Transactions on Pattern Analysis and Machine Intelligence*, vol. 19, no. 7, pp. 711–720, 1997.

[11] B. Moghaddam, "Principal manifolds and probabilistic subspaces for visual recognition," *IEEE Transactions on Pattern Analysis and Machine Intelligence*, vol. 24, no. 6, pp. 780–788, 2002.

[12] X. He, S. Yan, Y. Hu, P. Niyogi, and H. J. Zhang, "Face recognition using laplacianfaces," *IEEE Transactions on Pattern Analysis and Machine Intelligence*, vol. 27, no. 3, pp. 328–340, 2005.

[13] F. De la Torre and M. J. Black, "Robust principal component analysis for computer vision," in *IEEE International Conference on Computer Vision*. IEEE, 2001, vol. 1, pp. 362–369.

[14] E. J. Candès, X. Li, Y. Ma, and J. Wright, "Robust principal component analysis?," *Journal of the ACM (JACM)*, vol. 58, no. 3, pp. 11, 2011.

[15] F. De la Torre and M. J. Black, "A framework for robust subspace learning," *International Journal of Computer Vision*, vol. 54, no. 1-3, pp. 117–142, 2003.

[16] Q. Ke and T. Kanade, "Robust l_1 norm factorization in the presence of outliers and missing data by alternative convex programming," in *IEEE Conference on Computer Vision and Pattern Recognition*. IEEE, 2005, vol. 1, pp. 739–746.

[17] S. Li and J. Lu, "Face recognition using the nearest feature line method," *IEEE transactions on neural networks*, vol. 10, no. 2, pp. 439–443, 1999.

[18] J. Chien and C. Wu, "Discriminant waveletfaces and nearest feature classifiers for face recognition," *IEEE Transactions on Pattern Analysis and Machine Intelligence*, vol. 24, no. 12, pp. 1644–1649, 2002.

[19] K. Lee, J. Ho, and D. Kriegman, "Acquiring linear subspaces for face recognition under variable lighting," *IEEE Transactions on pattern analysis and machine intelligence*, vol. 27, no. 5, pp. 684–698, 2005.

[20] I. Naseem, R. Togneri, and M .Bennamoun, "Linear regression for face recognition," *IEEE Transactions on Pattern Analysis and Machine Intelligence*, vol. 32, no. 11, pp. 2106–2112, 2010.

This article has been accepted for publication in a future issue of this journal, but has not been fully edited. Content may change prior to final publication. Citation information: DOI 10.1109/TIFS.2018.2849883, IEEE Transactions on Information Forensics and Security

11

[21] X. Jiang and J. Lai, "Sparse and dense hybrid representation via dictionary decomposition for face recognition," *IEEE Transactions on Pattern Analysis and Machine Intelligence*, vol. 37, no. 5, pp. 1067–1079, 2015.

[22] J. Wright, A. Y. Yang, A. Ganesh, S. S. Sastry, and Y. Ma, "Robust face recognition via sparse representation," *IEEE Transactions on Pattern Analysis and Machine Intelligence*, vol. 31, no. 2, pp. 210–227, 2009.

[23] Z. Zhou, A. Wagner, H. Mobahi, J. Wright, and Y. Ma, "Face recognition with contiguous occlusion using markov random fields.," in *IEEE International Conference on Computer Vision*, 2009, pp. 1050–1057.

[24] A. Wagner, J. Wright, A. Ganesh, Z. Zhou, H. Mobahi, and Y. Ma, "Toward a practical face recognition system: Robust alignment and illumination by sparse representation," *IEEE Transactions on Pattern Analysis and Machine Intelligence*, vol. 34, no. 2, pp. 372–386, 2012.

[25] H. Zhang, J. Yang, Y. Zhang, N.M. Nasrabadi, and T.S. Huang, "Close the loop: Joint blind image restoration and recognition with sparse representation prior," in *IEEE International Conference on Computer Vision*. IEEE, 2011, pp. 770–777.

[26] M. Yang, L. Zhang, X. Feng, and D. Zhang, "Fisher discrimination dictionary learning for sparse representation," in *IEEE International Conference on Computer Vision*. IEEE, 2011, pp. 543–550.

[27] P. W. Holland and R. E. Welsch, "Robust regression using iteratively reweighted least-squares," *Communications in Statistics-theory and Methods*, vol. 6, no. 9, pp. 813–827, 1977.

[28] M. Yang, L. Zhang, J. Yang, and D. Zhang, "Robust sparse coding for face recognition," in *IEEE Conference on Computer Vision and Pattern Recognition*. IEEE, 2011, pp. 625–632.

[29] M. Yang, L. Zhang, J. Yang, and D. Zhang, "Regularized robust coding for face recognition," *IEEE Transactions on Image Processing*, vol. 22, no. 5, pp. 1753–1766, 2013.

[30] R. He, W. Zheng, B. Hu, and X. Kong, "A regularized correntropy framework for robust pattern recognition," *Neural computation*, vol. 23, no. 8, pp. 2074–2100, 2011.

[31] R. He, W. Zheng, and B. Hu, "Maximum correntropy criterion for robust face recognition," *IEEE Transactions on Pattern Analysis and Machine Intelligence*, vol. 33, no. 8, pp. 1561–1576, 2011.

[32] W. Deng, J. Hu, and J. Guo, "Extended src: Undersampled face recognition via intraclass variant dictionary," *IEEE Transactions on Pattern Analysis and Machine Intelligence*, vol. 34, no. 9, pp. 1864–1870, 2012.

[33] J. Lai and X. Jiang, "Class-wise sparse and collaborative patch representation for face recognition," *IEEE Transactions on Image Processing*, vol. 25, no. 7, pp. 3261–3272, 2016.

[34] W. Deng, J. Hu, and J. Guo, "In defense of sparsity based face recognition," in *IEEE Conference on Computer Vision and Pattern Recognition*, 2013, pp. 399–406.

[35] Y. F. Wang, C. P. Wei, and C. F. Chen, "Low-rank matrix recovery with structural incoherence for robust face recognition," in *IEEE Conference on Computer Vision and Pattern Recognition*. IEEE, 2012, pp. 2618–2625.

[36] Y. Zhang, Z. Jiang, and L. S. Davis, "Learning structured low-rank representations for image classification," in *IEEE Conference on Computer Vision and Pattern Recognition*, 2013, pp. 676–683.

[37] D. Bertsekas, *Constrained optimization and Lagrange multiplier methods*, Academic press, 2014.

[38] K. C. Lee, J. Ho, and D. J. Kriegman, "Acquiring linear subspaces for face recognition under variable lighting," *IEEE Transactions on Pattern Analysis and Machine Intelligence*, vol. 27, no. 5, pp. 684–698, 2005.

[39] R. Gross, I. Matthews, J. Cohn, T. Kanade, and S. Baker, "Multipie," *Image and Vision Computing*, vol. 28, no. 5, pp. 807–813, 2010.

[40] A. M. Martinez, "The AR face database," *CVC Technical Report*, vol. 24, 1998.

[41] G. B. Huang, M. Ramesh, T. Berg, and E. Learned-Miller, "Labeled faces in the wild: A database for studying face recognition in unconstrained environments," Tech. Rep., Technical Report 07-49, University of Massachusetts, Amherst, 2007.

[42] G. B. Huang, M. Mattar, H. Lee, and E. Learned-Miller, "Learning to align from scratch," in *Advances in Neural Information Processing Systems*, 2012, pp. 764–772.

Shicheng Yang received the B.S. degree in computer science and technology from Shandong Agricultural University, Tai'an, China, in 2015. He is currently working towards the M.S. degree in the Department of Computer Science and Technology, East China Normal University, Shanghai, China. His current research interests include pattern recognition, image processing, and especially face recognition.

Le Zhang received the B.E. degree in computer science and technology from Shanghai Institute of Technology, Shanghai, China, in 2013, and the M.S. degree in Pattern Recognition and Intelligent Systems at East China Normal University, Shanghai, China, in 2017. His research interests include pattern recognition and image processing.

Lianghua He received the B.S. degree in surveying and mapping from Wuhan Technical University of Surveying and Mapping, Wuhan, China, in 1999, the M.S. degree in surveying and mapping from Wuhan University, Wuhan, in 2002, and the Ph.D. degree in Signal and Information Processing from Southeast University, Nanjing, China, in 2005. From 2005 to 2007, he was a postdoctoral at Tongji University ,Shanghai, China. Since 2007, he has been with the Department of Computer Science and Technology, Tongji University, where he is currently a professor. His current research interests include medical image processing, machine learning.
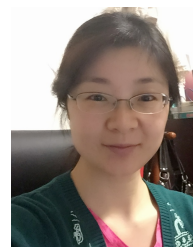
Ying Wen received the B.S. degree in industry automation from Technology of Hefei University in 1997 and the M.S. and Ph.D. degrees in imaging processing and pattern recognition from Shanghai University and Shanghai Jiao Tong University, China, in 2002 and 2009 respectively. She did research as a Postdoctoral Research Fellow at Columbia University in the city of New York from 2009 to 2011. She currently is a professor at East China Normal University. Her research interests include documentary processing, pattern recognition, machine learning and medical image processing.